ORNL/TM-2022/2574

# Considerations of Radiation-Hardened Electronics for Alpha Detectors in Molten Salt Reactors


K. C. Goetz
Kyle Reed
Neil Taylor
N. Dianne Bull Ezell

**Approved for public release.**
**Distribution is unlimited.**

**September 2022**

OAK RIDGE National Laboratory

ORNL IS MANAGED BY UT-BATTELLE LLC FOR THE US DEPARTMENT OF ENERGY

**ORNL/TM-2022/2574**

Nuclear Energy and Fuel Cycle Division
Electrification and Energy Infrastructure Division
Radioisotope Science and Technology Division

# Considerations of Radiation-Hardened Electronics for Alpha Detectors in Molten Salt Reactors

K. C. Goetz
F. Kyle Reed
Neil Taylor
N. Dianne Bull Ezell

Date Published: September 2022

Prepared by
OAK RIDGE NATIONAL LABORATORY
Oak Ridge, TN 37831-6283
managed by
UT-Battelle LLC
for the
US DEPARTMENT OF ENERGY
under contract DE-AC05-00OR22725

## CONTENTS

## LIST OF FIGURES

## ABBREVIATIONS

| | |
|---|---|
| ADC | analog-to-digital converter |
| ASIC | application-specific integrated circuit |
| CMOS | complementary metal oxide semiconductor |
| COTS | commercial-off-the-shelf |
| EMI | electromagnetic interference |
| FLiBe | lithium-fluoride beryllium-fluoride salt |
| FPGA | field programmable gate array |
| GaN | gallium nitride |
| HEMT | high electron mobility transistor |
| IC | integrated circuit |
| JFET | junction-gate field-effect transistor |
| MCA | multi-channel analyzer |
| MCNP | Monte Carlo N-Particle |
| MOSFET | metal-oxide-semiconductor field-effect transistor |
| MSBR | molten salt breeder reactor |
| MSR | molten salt reactor |
| PSRR | power supply rejection ratio |
| rad-hard | radiation-hardened |
| RHBD | radiation-hardening by design |
| RHBP | radiation-hardening by process |
| SEB | single-event burnout |
| Si | silicon |
| SiC | silicon carbide |
| SNM | special nuclear material |
| SNR | signal-to-noise ratio |
| SoA | state-of-the-art |
| TID | total ionizing dose |
| TMR | triple-modular redundancy |
| TRL | technology readiness level |
| VLSI | very large-scale integrated |
| WBG | wide bandgap |

# 1. INTRODUCTION

## 1.1 Motivation

Along with advanced generations of reactors quickly becoming reality, the need for instrumentation to provide reliable information for their safety and operation is also becoming relevant. Instrumentation-wise, molten salt reactors (MSRs) represent an especially challenging case in which detectors must survive extreme temperatures, high amounts of radiation, and a highly corrosive coolant. Adding to the complexity, tight material control and accounting must be maintained with any special nuclear material (SNM), a practice made more difficult by the nature of a loop of flowing fuel.

Alpha spectroscopy offers a unique window into investigating the isotopic concentrations of actinides within just such a molten salt environment. The characteristic $\alpha$ emissions of specific actinide isotopes in the salt enable quantification of their concentrations. Semiconductor devices based on wide bandgap materials such as silicon carbide and gallium oxide can withstand the extreme temperatures within MSRs and offer good chemical stability with the corrosive salt. Collaborators at The Ohio State University are fabricating and testing a $\beta$ gallium oxide $\alpha$ particle sensor that could identify actinide concentrations within the fuel salt to help improve the material control and accounting required for complicated system inherent to MSRs.

## 1.2 Potential Users

Several reactor developers will benefit from development of this detector. FLiBe Energy, Kairos Power, and Alpha Technologies are all developing MSRs that require instrumentation for salt species tracking. A comprehensive understanding of the thermophysical and thermochemical properties, species tracking, and monitoring corrosion development will directly impact the performance of an MSR.

## 1.3 Effects of Radiation on Electronics

Alpha spectroscopy signals typically occur on the order of ~10 nA. These small signals are easily lost in lengthy cabling, and the electronics required to support alpha detectors must be placed in close proximity to their supporting electronics to have an adequate signal-to-noise ratio (SNR).

Semiconducting electronic devices degrade as a result of high temperature and radiation. Neutron radiation has multiple damaging effects that will impact the performance of electronics. Neutrons displace the atoms within the lattice structure, creating defects, increasing resistivity, reducing carrier lifetimes, and activating the material through neutron capture. In the case of silicon, $\beta$ decay post neutron capture will create phosphorus, thus increasing the dopant profile of the material while also releasing $\beta$ particles and $\gamma$ rays.

Ionizing radiation generates electron hole pairs along its incident path. This creates charge trapping centers in the insulating materials and overlays of semiconducting devices, thus influencing their operation through changes in threshold voltages and leakage currents. Single-event upsets are introduced through the rapid accumulation of charges and currents in devices, thus creating transient errors flipping the Boolean logic

states of digital systems. Wide bandgap semiconducting materials such as silicon carbide (SiC) and gallium nitride (GaN) have been of particular interest in the radiation-hardened electronics community because of (1) the higher energy required to excite electrons from the valence band to the conduction bands and (2) the increased voltage breakdowns. These factors support the impetus for increased semiconductor doping. SiC-based metal-oxide-semiconductor field-effect transistors (MOSFETs) and junction-gate field-effect transistors (JFETs) have been shown to increase their resistance to neutron fluence by an order of magnitude over silicon (Si)-based devices [1]. However, SiC-based power MOSFETs have decreased neutron ratings as a result of associated single-event burnouts from ionization trails [2–6]. GaN-based high electron mobility transistors (HEMTs) have been shown to tolerate roughly twice the total ionizing dose (TID) of comparable Si devices [7–11].

## 2. MSR ENVIRONMENT

A detailed neutronics model of a conceptual design of a MSBR was recently completed to analyze the biological neutron dose rate in the reactor cell [12]. This model represents one of the best estimates for the expected neutron flux values for instrumentation and electronics and is the assumed reactor model for this report. Figures 1 and 2 show the MSBR cell and heat exchangers [12].

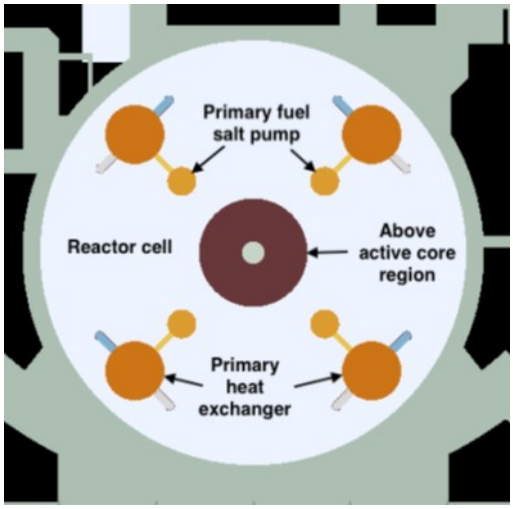


**Figure 1. MSBR cell area with heat exchangers and salt pumps.**

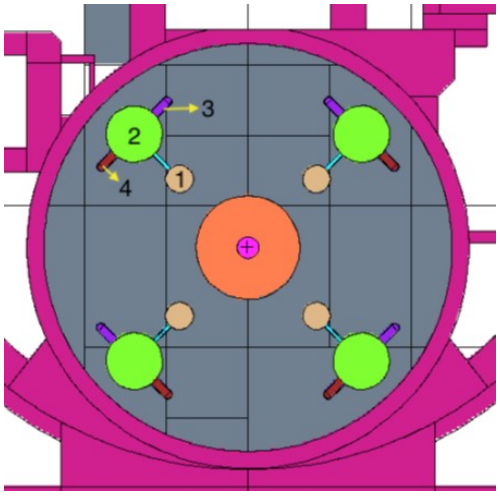


**Figure 2. Radial view of MCNP model of MSBR cell. Region 1 shows the fuel salt exiting the pump, Region 2 shows the homogenized mixture of fuel and coolant within the heat exchanger, and Regions 3 and 4 show the hot and cold legs of the coolant salt.**

The modeling process determined the expected neutron flux and biological dose rates in and around the reactor cell. The values of the neutron flux for the gallium oxide $\alpha$ sensor and electronics were obtained from the edge of one of the heat exchangers, as shown in Figure 3 [12].

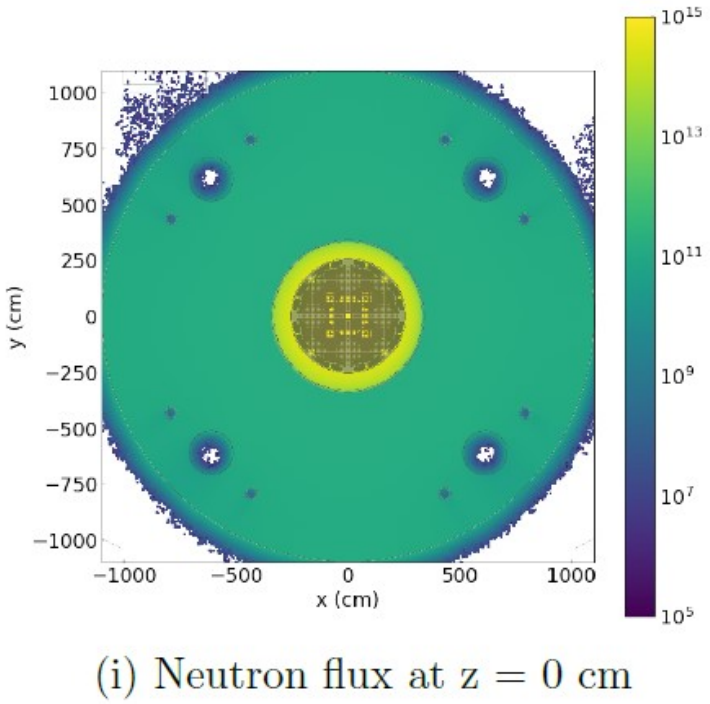


**Figure 3. Neutron flux ($n/cm^2 \cdot s$) at core center plane.**

These values range from ~$10^5$–$10^9$ depending on the exact placement within the heat exchanger. The gallium oxide sensors themselves will be in contact with the fuel salt for measurement purposes, thus it is assumed that the device will experience the greatest flux value of $10^9$ n/(cm$^2$·s).

In general, if it is assumed that the damage in gallium oxide is approximately equal to the damage in SiC, then the devices will reach $10^{14}$ n/cm$^2$ in ~1 day and $10^{16}$ n/cm$^2$ in ~230 days.

In addition to neutrons, the detector will also be experiencing high levels of $\gamma$, $\alpha$, and $\beta$ radiation. The relative fluxes experienced by the device will be influenced by the fission products within the fuel salt as well as the detector's placement. Argonne National Laboratory is currently conducting a detailed analysis for $\gamma$ rays similar to that conducted for neutronics modeling. The $\alpha$ flux will contribute some to the device's radiation damage, depending on the flux, but it will also impact the device's sensor performance. Semiconductor detectors require a refractory period after an event during which charges move out of the depletion region in the device. If a second pulse arrives before the end of this period, the detector will not be able to differentiate between events resulting in an effect called pile-up. As most acquisition systems reject pile-up events whenever possible so as not to create erroneous peaks in the spectrum, this results in detector dead time. Therefore, if the $\alpha$ flux is too high then the device will experience significant dead time and pulse pile up that will degrade the sensor's resolution and ability to determine isotopic concentration.

## 3. PATH TO TEMPERATURE AND RADIATION-HARDENED FRONT END ELECTRONICS

### 3.1 Radiation Effects on Electronics

Both ionizing radiation and neutron bombardment influence material conductivity, leading to variations in electronic component parameters and parasitics. Ionizing radiation increases the conductivity of materials through free carrier production. Increased conductivity leads to increased leakage currents across dielectric (insulating) materials, which in turn leads to decreases of SNR across lengthy cables and second-order changes in the dielectric constant of capacitors. Through the displacement of atoms in a material's lattice structure, neutrons decrease the conductivity of the material. Decreased conductivity (increased resistivity) results in power losses in lengthy cables.

In general, passive components are relatively resistant to radiation effects. Resistors may have minor variations in conductivity as a result of radiation, but these are typically within the standard device's tolerances. $\gamma$ heating has a greater effect on the performance of passive components. Capacitors with large temperature coefficients can have large variations in capacitance when thermal expansion changes their geometry. Of passive devices, capacitors are the most sensitive to radiation effects and have been shown to vary by greater than 20% for a 1 MGy TID [13].

Modern electronics applications do not rely on passive devices alone: they also require amplifiers, switches, and nonlinear devices. These basic electronic devices are built from solid-state semiconductors. Semiconductors are the prominent point-of-failure in irradiated electronics circuits. An electronics engineer must consider semiconductor physics and radiological effects, susceptibilities, and the limits of semiconductors respective of the intended radiological environment. In brief, Table 1 provides an overview of the neutron degradation of selected discrete active devices through the associated device fluence limits and the displacement damage effects on the present state-of-the-art (SoA) devices. Similarly, Table 2 summarizes the $\gamma$-accumulated dose effects on devices and their respective TID limits. The information in these tables addresses the maximum limits of these devices: not all devices in a category will survive these limits, and not all will be useful for every application. More information on device physics, radiation failure mechanisms, and limits can be found in the literature [14, 15].

**Table 1. Neutron displacement damage on Si device technologies [14]**

| Type | Max fluence ($n/cm^2$) | Displacement effects |
|---|---|---|
| Diodes | $10^{13}$ – $10^{15}$ | Increased leakage currents, increased forward voltage threshold |
| LEDs | $10^{12}$ – $10^{14}$ | Reduced light intensity |
| BJTs | $10^{13}$ | Current gain degradation |
| JFETs | $10^{14}$ | Increased channel resistivity, decreased carrier mobilities |
| MOSFETs | $10^{15}$ | Increased channel resistivity, decreased carrier mobilities |
| CMOS | $10^{15}$ | Increased channel resistivity, decreased carrier mobilities |

**Table 2. Gamma TID damage on Si device technologies [14]**

| Type | TID (Gy) | TID Effects |
|---|---|---|
| Photodiodes | $10^4$ – $10^6$ | Increased photocurrents |
| LEDs | $10^5$ – $10^6$ | 0.25 dB attenuation |
| BJTs | $10^3$ – $10^5$ | Current gain degradation and increased leakage currents |
| JFETs | $>10^6$ | Minimal observable effects |
| MOSFETs | $10^4$ | Increasing threshold voltage and leakage currents |
| CMOS | $10^6$ | Variations in threshold voltage and leakage currents |

### 3.2 Pathways to Rad-Hard Electronic Systems

The roadmap (see Figure 4) for radiation-hardened (rad-hard) uses in reactor environments has three possible paths: use of *space-rated* electronics, *component-wise* design through the use of commercial-off-the-shelf (COTS) components without a radiation rating but with good chances for survival (such as JFETs), or development of *fully custom* rad-hard application-specific integrated circuit (ASIC) design.

**Space-rated components** have high technology readiness levels (TRLs) and are commercially available, but they are typically irradiated to 3–10 kGy (Si) and rarely have any rated neutron limits. Because of their availability, the design time and associated costs are relatively low. However, the device behavior under irradiation, which is particularly critical for analog circuitry, may be omitted from their data sheets. Performance of the necessary irradiation and associated verification procedures will result in significant increases in system development costs.

**Component-wise systems** are developed by using COTS components with intrinsic radiation-resistant properties. For instant, JFETs, which do not have gate insulation, have withstood >1 MGy (Si) [1, 16, 17]. Intrinsically radiation-resistant components can be leveraged to develop a lower cost solution with a radiation tolerance that is orders of magnitude greater than space-rated solutions. The design time required for these systems and the associated costs can be low. However, the systems will require multiple irradiation evaluations at the device and circuit levels, and the physical dimensions of the solution can be quite large. This may result in multiple design iterations to locate suitable components or to compensate for radiation effects.

Designing **fully custom rad-hard electronic integrated circuits (ICs)**, ranging from small-scale to very large-scale integrated (VLSI) circuits, yields the greatest radiation (and temperature) tolerance for electronic systems by using radiation-hardening by design (RHBD) and radiation-hardening by process (RHBP) techniques. RHBD techniques consist of design principles on the architectural, circuit, and layout levels, and they may incorporate redundancy and voting schemes such as triple-modular redundancy (TMR) or error correction codes to reduce soft (recoverable) errors typically caused by large transient radiation [18–20].

RHBP focuses on device construction and the materials used in the fabrication process that increase radiation resistance. Gate oxides, shallow-trench-isolation islands, and spacing oxides are susceptible to charge trapping [21] and must be avoided in rad-hard electronics processes. Small feature size complementary metal oxide semiconductor (CMOS) processes have led to an increase in the TID of Si semiconductors and ICs to 10 MGy [21]. Wide bandgap (WBG) semiconducting materials have been shown to withstand TIDs similar to that of Si JFETs, with an increase of neutron fluence rating of 1–2 orders of magnitude [1, 7, 9, 10, 22–24]. This pathway is has the highest costs for design time and prototyping because it starts from a foundation-

ally low TRL. However, this design approach can produce circuits and systems with very high radiation resistance at a low fabrication cost for reasonable volume production.

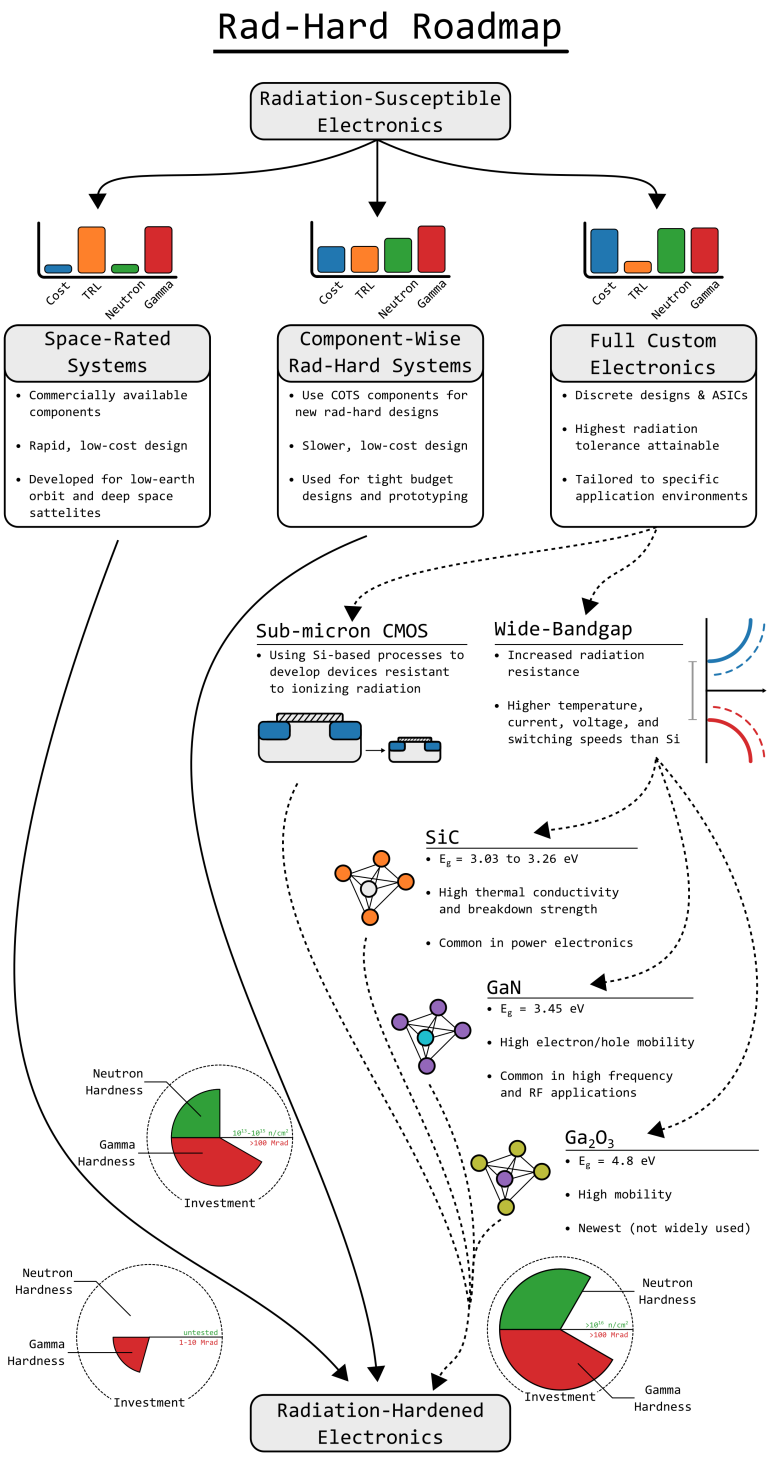


**Figure 4. Pathways to develop radiation-hardened electronic systems [25].**

# 4. SCHOTTKY ALPHA DETECTOR

## 4.1 Principles of Operation

Semiconductor detectors, sometimes referred to as *solid state detectors*, generate most of their signal from ionization events that create electron-hole pairs along the path of incident radiation [26]. These electron-hole pairs are swept to contacts where they are collected by the internal and external applied electric fields. Schottky radiation detectors are composed of several effective layers, as shown in Figure 5 [27]. The depletion region (green) is the active detection region of the device. Its width is controlled by the bias voltage denoted by $V_{bias}$. Diode detectors operate in the same manner as Schottky diodes, with a depletion region formed by the exchange of charge carriers created by the differences in doping concentration within the semiconductor.

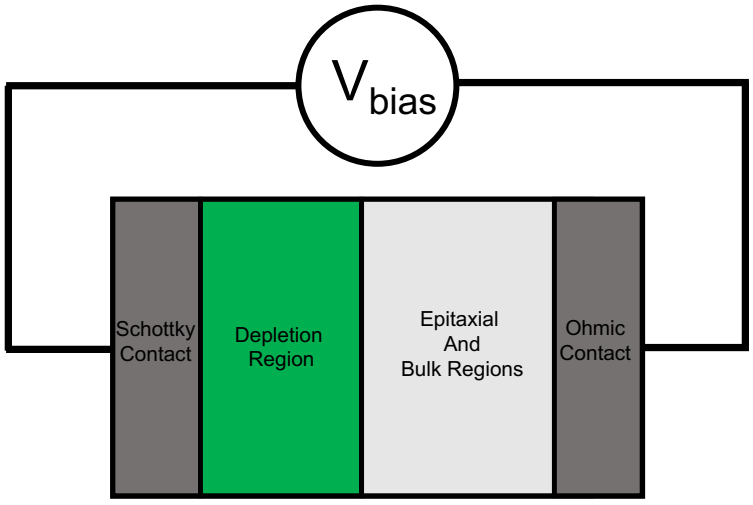


**Figure 5. Diagram of a Schottky semiconductor detector outlining the effective regions in the device. The depletion region (green) is the device's active detection region, the width of which is controlled by $V_{bias}$.**

The depletion region acts as the effective sensing volume of the detector; therefore, all of the radiation energy should ideally be deposited within this region for detection. Some small amounts of diffusion current outside this region can be collected, but the charge diffusion lengths can vary for each device based on the material and defect concentrations. The depletion region should be maximized to ensure that the incident $\alpha$ particles are completely stopped within the region and that the metal contacts are minimized to reduce attenuation of the $\alpha$ particles. Because $\alpha$ particles are positively charged, they are highly interactive with the electron clouds surrounding atoms and therefore have a very short path length through matter. For gallium oxide, the expected range of a 5.486 MeV $\alpha$-particle is approximately 14 microns, whereas the range of the same energy $\alpha$ in SiC is 18.9 microns [27]. The implication is a thin detector will be highly efficient with a minimum probability of $\alpha$ particle escape.

## 4.2 Options for Implementation

The short range of $\alpha$ particles presents a challenge with the implementation of an $\alpha$ detector in a molten salt environment. An $\alpha$ particle sensor must be exposed directly to the salt to perform actinide measurements. As such, appropriate feedthroughs will be required to position the device so that the sensor face is immersed in the salt. These types of devices have shown success in operation at elevated temperatures (500 °C) and while immersed in molten salt [28, 29]. The high linear energy transfer coefficient of $\alpha$ particles also results in strong self-shielding effects. The self-shielding causes a significant broadening in the observed energy spectrum. A broadened spectrum makes it difficult or impossible to resolve between $\alpha$ particles of different energies, compromising the detectors ability to determine the isotopic concentration of molten salt. One possible solution is to use a small salt channel off the side of the main molten salt pipe, which would serve to greatly reduce the source thickness. Additional system longevity could be achieved if the smaller salt channel were used alongside shielded electronics.

To increase the efficiency of any end detector, the volume of the detection region must be maximized. Should more detection efficiency be required, a pixelated detector array could be used to increase the effective detection area of the sensor, as shown in Figure 6.

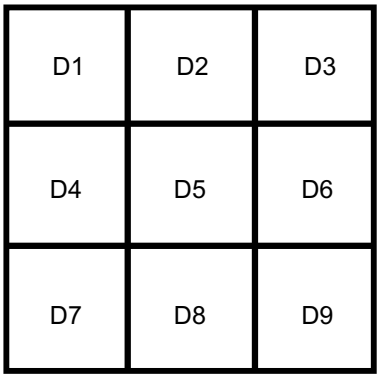


**Figure 6. Diagram of a pixelated Schottky semiconductor detector: D1, D2, etc., depict individual diodes.**

Semiconductor detectors such as Schottky diodes are not only sensitive to $\alpha$ radiation. They are also sensitive to x-ray, $\beta$, $\gamma$, and neutron radiation, all of which will be present in varying magnitudes in an MSR environment. These other forms of ionizing radiation could impact the deadtime and noise floor of the sensor, depending on the magnitude of the other radiation sources. Possible solutions to this dilemma take advantage of the short penetration depth of $\alpha$ particles. One method is to have a purposefully thin detector and tune the depleted region's depth to $\alpha$ particles specifically. Because the other forms of radiation outlined above are more penetrating, many of them will not be fully stopped within the active region of the detector. A second option is to use multiple diodes, perhaps in the similar tiled configuration as shown in Figure 6, with some of the diodes coated in a medium to block $\alpha$ radiation while still being permissive to other radiation types. These blocked diodes could then be used as background subtraction.

If device background proves to be problematic and high event rates are troublesome, pixelated detectors could be combined with background subtraction tiles with other $\gamma$ ray detectors. If this composite detector is placed in a ring around the beam pipe, then it could be used to detect $\alpha$-$\gamma$ coincidences as a form of active

background rejection. Of course, the $\alpha$ detection portion of the detector would need to be in contact with the molten salt, but the $\gamma$ detection portion would not have such a requirement.

### 4.3 Detector Location

A suitable location for the detector system could be on the cold leg of the molten salt loop, on the cold side of the heat exchanger. Temperatures would be slightly lower there, thus boosting system longevity, and dose rates would also be lower on the periphery away from the core. For lithium-fluoride beryllium-fluoride salt (FLiBe) specifically, this temperature would be int he range of 400–500 °C, which is a significant decrease from 800 °C.

# 5. ACQUISITION ELECTRONICS

## 5.1 Conventional Acquisition Systems

Detectors meant for spectroscopy are traditionally read out by a fast charge sensitive pre-amplifier, the basic diagram of which is shown in Figure 7. This serves to amplify and convert the signal from a current pulse to a voltage pulse and to boost SNR. If the acquisition is analog, then the signal is then shaped with a shaping amplifier which produces an output voltage pulse with a height proportional to the area of the input voltage pulse. This will also improve the SNR by removing high-frequency noise at the cost of significantly increased instrument dead-time and consequentially missed events. The signal may then be read in by a multi-channel analyzer (MCA). If digital acquisition is preferred, then the signal is sent directly from the pre-amplifier to a digitizer, which is composed of an analog-to-digital converters (ADCs) and a field programmable gate array (FPGA). The signal is then shaped within the FPGA with a trapezoidal filter. Digital shaping serves the same purpose as with a shaping amplifier, providing an ADC value proportional to the area underneath the incoming pulse. Digital acquisition has the benefit of being more a compact, lower dead-time system capable of reading in and time correlating many channels simultaneously.

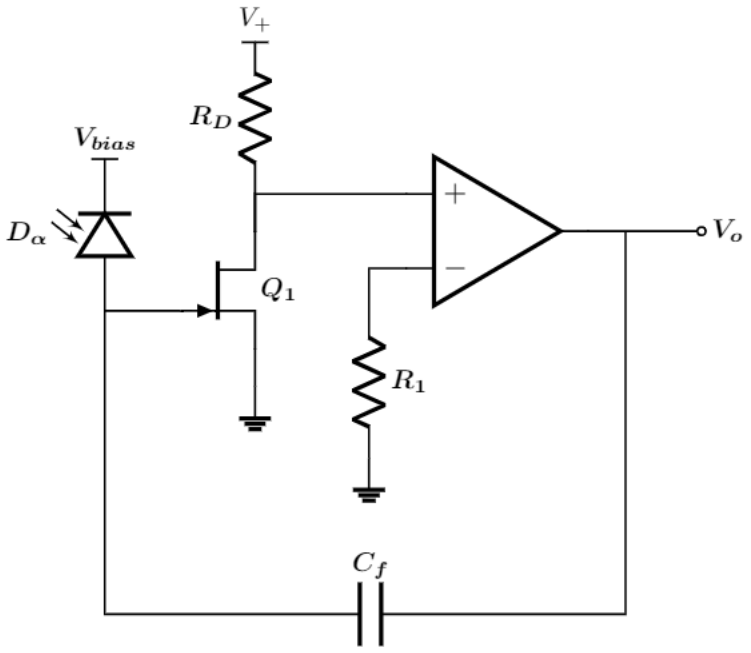


**Figure 7. Circuit diagram of a charge sensitive preamplifier.**

## 5.2 Recommendations

### 5.2.1 Acquisition Layout/Location

Because of the short distance $\alpha$ particles travel through matter, the $\alpha$ detector itself must be in contact with the molten salt. SiC detectors have shown success with immersion of a 550 °C molten salt environment,

successfully operating as an $\alpha$ detector after being withdrawn from the environment [28, 29]. The output of the detector will pass through a feed-through in the side of the pipe to a shielded box a short distance away. The shielded box will host JFET-based pre-amplifiers and possibly high voltage power supplies for each detector channel. The pre-amplified signal from the detector will then be sent to a digital acquisition system located some safe distance away in a low-radiation low-temperature area.

Close placement of the pre-amplifier electronics to the $\alpha$ detector diode is critical. The charge from the detector would easily be lost in the noise of a lengthy cable as a result of electromagnetic interference (EMI) and capacitive cable parasitics. However, the pre-amplifier noise will increase with increasing temperature, radiation dose, and dose rate. Better radiation modeling of electronics to the radiation profile of the reactor location is required to determine the optimum placement of the pre-amplifier electronics.

### 5.2.2 Pre-amplifier Specifications

For minimum signal fidelity, a charge-sensitive pre-amplifier must have pole-zero correction, a gain of at least 90 mV/MeV, and a rise time of less than 50 ns [27]. Given the speed of semiconductor detectors, possible length of cabling, and the desire to have multiple channels, more amplification and digital acquisition is highly recommended.

Because of the number of $\alpha$ particles produced in fueled salt and the refractory period that semiconductor detectors require to reform the depletion region, the event rate of the detectors might be very high. In this case, a large amount of pile-up events that are indistinguishable from one another would occur, thus resulting a poor $\alpha$ spectrum. If this proves to be the case, then it could be beneficial to include $\gamma$ ray detectors in the system. The detector array would then be examining the molten salt for $\alpha$-$\gamma$ coincidences. Therefore, the rate could be reduced through a hardware coincidence requiring an $\alpha$ channel and a $\gamma$ channel to collect an event within a small window of time to send data to the digitizer.

### 5.2.3 Diode Biasing Circuitry

Diode bias voltage not only sets the width of the sensitive region of the device, but it also sets the gain. The result from the perspective of the measured spectrum is that bias voltage sets calibration. Therefore, changes to bias voltage such as drift or ripple will have the highly undesirable effect of changing calibration coefficients mid measurement. Power supply ripple in particular would degrade the spectrum, thus resulting in broadened peaks and consequent loss of detector resolution. Standard bias voltages for devices of this type range from 60–200 V, with 2–20 mV from peak to peak of ripple. Current draw ranges from from 20–300 μA [27]. Bias voltage is usually adjustable to optimize the SNR, to occupy as much of the bit-depth of the ADC as possible, and/or to set a desired calibration.

Power electronics used to supply power to the detector diode may be more susceptible to neutrons than to ionizing radiation. Recent research has shown that SiC power transistors (typically MOSFETs or JFETs because of their low "on" resistance and rapid switching speeds) suffer from neutron single-event burnouts (SEBs) limiting their fluence to $\leq 10^5$–$10^9$ n/cm$^2$ [2–5]. SEBs are believed to occur from currents induced by recoil ionization trails from neutron absorption in the semiconductor [6]. Placement of these power electronics must consider the sensitivity of the power electronic architecture to the radiation profile. When using Si- or SiC-based electronics such as a boost converter with low ripple voltage (or followed by a linear regulator with high power supply rejection ratio (PSRR)), a location with lower neutron fluence is required.

## 6. CONCLUSIONS AND FUTURE WORK

Reactor operation stability requires accurate, reliable instrumentation that is strategically placed to obtain the maximum information for safe controls. Radiation detection in molten salt reactors for species tracking is required throughout the system. However, sensor longevity and performance are limited because of corrosion, high temperatures, and high radiation. The $\alpha$ sensor and electronics discussed herein represent one proposed solution for species tracking on the cold leg of the molten salt loop. This location was selected because of the lower temperature (400–500 °C) with the presence of radiation. Although this temperature is significantly decreased from the expected reactor core temperatures, it is still extreme for commercially available electronics. The recommendation presented here is to couple radiation-hardening-by-design techniques with wide bandgap materials to enable installation of readout electronics very close to the $\alpha$ sensor. Conventional data acquisition systems for $\alpha$ sensors require a charge-sensitive pre-amplifier that can be built using JFETS and diodes.

Fabrication and demonstration of this system would require additional funding but would be impactful, surpassing one of the current limitations for nuclear instrumentation in advanced reactors.

## 7. REFERENCES


[1] J. McGarrity, F. McLean, W. DeLancey, J. Palmour, C. Carter, J. Edmond, and R. Oakley, "Silicon Carbide JFET Radiation Response," *IEEE Transactions on Nuclear Science*, vol. 39, no. 6, pp. 1974–1981, 1992.

[2] D. J. Lichtenwalner, A. Akturk, J. McGarrity, J. Richmond, T. Barbieri, B. Hull, D. Grider, S. Allen, and J. W. Palmour, "Reliability of SiC Power Devices against Cosmic Ray Neutron Single-Event Burnout," in *Materials Science Forum*, vol. 924. Trans Tech Publ, 2018, pp. 559–562.

[3] A. Akturk, R. Wilkins, J. McGarrity, and B. Gersey, "Single Event Effects in Si and SiC Power MOSFETs due to Terrestrial Neutrons," *IEEE Transactions on Nuclear Science*, vol. 64, no. 1, pp. 529–535, 2016.

[4] C. Martinella, R. G. Alía, R. Stark, A. Coronetti, C. Cazzaniga, M. Kastriotou, Y. Kadi, R. Gaillard, U. Grossner, and A. Javanainen, "Impact of Terrestrial Neutrons on the Reliability of SiC VD-MOSFET Technologies," *IEEE Transactions on Nuclear Science*, vol. 68, no. 5, pp. 634–641, 2021.

[5] K. Rashed, R. Wilkins, A. Akturk, R. Dwivedi, and B. Gersey, "Terrestrial Neutron Induced Failure in Silicon Carbide Power MOSFETs," in *2014 IEEE Radiation Effects Data Workshop (REDW)*. IEEE, 2014, pp. 1–4.

[6] T. Shoji, S. Nishida, K. Hamada, and H. Tadano, "Analysis of Neutron-Induced Single-Event Burnout in SiC Power MOSFETs," *Microelectronics Reliability*, vol. 55, no. 9-10, pp. 1517–1521, 2015.

[7] M. Rahman, A. Al-Ajili, R. Bates, A. Blue, W. Cunningham, F. Doherty, M. Glaser, L. Haddad, M. Horn, J. Melone, M. Mikuz, T. Quinn, P. Roy, V. O'Shea, K. Smith, J. Vaitkus, and V. Wright, "Super-Radiation Hard Detector Technologies: 3-D and Widegap Detectors," *IEEE Transactions on Nuclear Science*, vol. 51, no. 5, pp. 2256–2261, 2004.

[8] F. Berthet, Y. Guhel, B. Boudart, H. Gualous, J. Trolet, M. Piccione, and C. Gaquiere, "Impact of Low Gamma Radiation Dose on Electrical Trap Related Effects in AlGaN/GaN HEMTs," *Electronics Letters*, vol. 48, no. 17, pp. 1078–1079, 2012.

[9] S. Pearton, F. Ren, E. Patrick, M. Law, and A. Y. Polyakov, "Ionizing Radiation Damage Effects on GaN Devices," *ECS Journal of Solid State Science and Technology*, vol. 5, no. 2, p. Q35, 2015.

[10] H. Von Bardeleben, J. Cantin, U. Gerstmann, A. Scholle, S. Greulich-Weber, E. Rauls, M. Landmann, W. Schmidt, A. Gentils, J. Botsoa *et al.*, "Identification of the Nitrogen Split Interstitial (N- N) N in GaN," *Physical Review Letters*, vol. 109, no. 20, p. 206402, 2012.

[11] J. Kim, B. L. Grisso, J. K. Kim, D. S. Ha, and D. J. Inman, "Electrical Modeling of Piezoelectric Ceramics for Analysis and Evaluation of Sensory Systems," in *2008 IEEE Sensors Applications Symposium*. IEEE, 2008, pp. 122–127.

[12] E. Davidson, G. Radulescu, K. Smith, J. Yang, S. Wilson, and B. R. Betzler, "Reactor Cell Neutron Dose For the Molten Salt Breeder Reactor Conceptual Design," *Nuclear Engineering and Design*, vol. 383, 2021.

[13] C. Hanks and D. Hamman, "Radiation Effects Design Handbook. Section 3. Electrical Insulating Materials and Capacitors," Battelle Memorial Inst., Columbus, Ohio. Radiation Effects Information Center, Tech. Rep., 1971.

[14] F. K. Reed, N. D. B. Ezell, M. N. Ericson, and C. L. Britton, Jr., "Radiation Hardened Electronics for Reactor Environments," 10 2020. [Online]. Available: https://www.osti.gov/biblio/1763473

[15] N. Ezell, K. Reed, and M. Ericson, "Radiation-Hard Electronics for Nuclear Instrumentation in Terrestrial Reactors," in *12th Nuclear Plant Instrumentation, Control and Human-Machine Interface Technologies (NPIC & HMIT 2021)*, 2021, pp. 556–563.

[16] F. K. Reed, M. N. Ericson, N. D. B. Ezell, R. A. Kisner, L. Zuo, Z. Haifeng, and R. Flammang, "A 100 Mrad (Si) JFET-Based Sensing and Communications System for Extreme Nuclear Instrumentation Environments," *Nuclear Technology*, 2022.

[17] F. K. Reed, "Radiation-Hardened Sensing and Communication Electronics with Frequency Drift Correction Using JFET Technology," Ph.D. dissertation, Tennessee Technological University, 2022.

[18] D. G. Mavis and D. R. Alexander, "Employing Radiation Hardness by Design Techniques with Commercial Integrated Circuit Processes," in *16th DASC. AIAA/IEEE Digital Avionics Systems Conference. Reflections to the Future. Proceedings*, vol. 1. IEEE, 1997, pp. 2–1.

[19] D. Lunardini, B. Narasimham, V. Ramachandran, V. Srinivasan, R. D. Schrimpf, and W. H. Robinson, "A Performance Comparison between Hardened-by-Design and Conventional-Design Standard Cells," in *RADECS 2004 Workshop*, 2004.

[20] A. Stabile, V. Liberali, and C. Calligaro, "Design of a Rad-Hard Library of Digital Cells for Space Applications," in *2008 15th IEEE International Conference on Electronics, Circuits and Systems*. IEEE, 2008, pp. 149–152.

[21] M. D. Matteis, F. Resta, A. Pipino, F. Fary, S. Mattiazzo, C. Enz, and A. Baschirotto, "1-Grad-TID Effects in 28-nm Device Study for Rad-Hard Analog Design," *Next-Generation ADCs, High-Performance Power Management, and Technology Considerations for Advanced Integrated Circuits*, pp. 299–315, 2020.

[22] J.-M. Lauenstein, P. G. Neudeck, K. L. Ryder, E. P. Wilcox, L. Chen, M. A. Carts, S. Y. Wrbanek, and J. D. Wrbanek, "Room Temperature Radiation Testing of a 500°C Durable 4H-SiC JFET Integrated Circuit Technology," in *2019 IEEE Radiation Effects Data Workshop*. IEEE, 2019, pp. 1–7.

[23] J.-M. Lauenstein, M. C. Casey, R. L. Ladbury, H. S. Kim, A. M. Phan, and A. D. Topper, "Space Radiation Effects on SiC Power Device Reliability," in *2021 IEEE International Reliability Physics Symposium (IRPS)*. IEEE, 2021, pp. 1–8.

[24] B. Tala-Ighil, J.-L. Trolet, H. Gualous, P. Mary, and S. Lefebvre, "Experimental and Comparative Study of Gamma Radiation Effects on Si-IGBT and SiC-JFET," *Microelectronics Reliability*, vol. 55, no. 9-10, pp. 1512–1516, 2015.

[25] K. Reed, C. Goetz, N. Ericson, D. Sweeney, and N. D. Ezell, "Wide Bandgap Semiconductors for Extreme Temperature and Radiation Environments," Oak Ridge National Lab.(ORNL), Oak Ridge, TN (United States), Tech. Rep., 2022.

[26] G. F. Knoll, *Radiation Detection and Measurement*. John Wiley & Sons, 2010.

[27] N. R. Taylor, "Evaluation of Metal Printing and Cleanroom Fabricated SiC and $Ga_2O_3$ Radiation Sensors," Ph.D. dissertation, The Ohio State University, 2021.

[28] J. Jarrell, "Fabrication and Characterization of a Silicon Carbide Alpha Detector for Molten Salt Application," Ph.D. dissertation, The Ohio State University, 2018.

[29] N. Taylor, N. Alnajjar, J. Jarrell, P. Kandlakunta, M. Simpson, T. Blue, and L. Cao, "Isotopic Concentration of Uranium from Alpha Spectrum of Electrodeposited Source on 4H-SiC Detector at 500°," *Journal of Radioanalytical and Nuclear Chemistry*, vol. 320, pp. 441–449, 2019.